

# Imaging in solution of (Lys)<sub>16</sub>-containing bifunctional synthetic peptide/DNA nanoparticles for gene delivery

Louise Collins<sup>a</sup>, Michael Kaszuba<sup>b</sup>, John W. Fabre<sup>a,\*</sup>

<sup>a</sup>Department of Clinical Sciences, Rayne Institute, King's Denmark Hill Campus, 123 Coldharbour Lane, London SE5 9NU, UK

<sup>b</sup>Malvern Instruments Limited, Enigma Business Park, Grovewood Road, Malvern, Worcestershire WR14 1XZ, USA

Received 1 July 2003; received in revised form 9 February 2004; accepted 11 February 2004

## Abstract

The physical properties of non-viral vector/DNA nanoparticles in physiological aqueous solution are poorly understood. A Fluid Particle Image Analyser (FPIA), normally used for analysis of industrial and environmental fluids, was used to visualise individual (Lys)<sub>16</sub>-containing peptide/DNA particles. Eight (Lys)<sub>16</sub>-containing synthetic peptides were used to generate peptide/DNA particles at a constant + to – charge ratio of 2.8:1 with 10 µg/ml of plasmid DNA in phosphate buffered saline. Dynamic Light Scattering (DLS) and gene delivery studies were also performed. We present the first images of non-viral vector/DNA nanoparticles in physiological aqueous solution, together with precise measurements of individual particle size and shape in solution and, for the first time, an accurate measure of particle number. Particle size and shape, particle number, and efficiency for gene delivery varied markedly with different peptides. Under standard conditions for in vitro gene delivery, we estimate ~ 60 peptide/DNA nanoparticles per target cell, each containing ~ 70,000 plasmids. This novel capacity to image individual vector/DNA nanoparticles in solution and to count them accurately will enable a more precise assessment of non-viral gene delivery systems, and a more quantitative interpretation of gene delivery experiments.

© 2004 Elsevier B.V. All rights reserved.

**Keywords:** Gene therapy; Vector/DNA nanoparticle; Synthetic peptide; DNA vector; Polylysine; Fluid Particle Image Analyser

## 1. Introduction

Virtually all non-viral gene delivery systems incorporate a polycation component (for reviews see Refs. [1–3]). This binds DNA phosphate groups electrostatically, and (once DNA charge is neutralised) the DNA collapses into nanoparticles which are more easily transported across plasma membranes. We have been developing bifunctional synthetic peptides as DNA vectors [4–11]. These incorporate a (Lys)<sub>16</sub> chain for electrostatic binding of DNA, and a short peptide sequence intended for targeting plasma membrane receptors. These peptides have several favourable properties, in particular the fact that they are based on the natural amino acid L-lysine and normal peptide bonds, and that they are readily standardized and essentially non-immunogenic.

The physical properties of vector/DNA nanoparticles in physiological aqueous solutions are a crucial factor for the

efficiency of gene delivery. Dynamic Light Scattering (DLS) has been the most frequently used technique, and provides a measure of the size distribution of particles in suspension (e.g. Ref. [10]). The mean diameter (the z-average diameter, Z<sub>Ave</sub>) is based on the intensity of scattered light and the width of the distribution (the polydispersity index) is a measure of particle uniformity. However, particles are assessed en bloc rather than individually, are assumed to be spherical, and the result is weighted by the presence of larger particles. Quantitative information cannot be obtained from this technique. Visualisation of individual nanoparticles using atomic force microscopy (e.g. Ref. [12]) or electron microscopy techniques (e.g. Ref. [13]) involves addition of salts and drying of solutions on to surfaces. Since the presence of salts and the concentration of DNA markedly influence the properties of vector/DNA nanoparticles [8,13,14], these studies are of uncertain relevance to the condition of the nanoparticles as encountered by target cells in physiological solutions. One study has used transmission electron microscopy on cells transfected with cationic lipid/DNA nanoparticles, to visualise the nanoparticles in intracellular compartments [15].

\* Corresponding author. Tel.: +44-20-7848-5141; fax: +44-20-7848-5143.

E-mail address: [john.fabre@kcl.ac.uk](mailto:john.fabre@kcl.ac.uk) (J.W. Fabre).

The precise assessment of particles in fluid suspension is a key component of quality control in many industries, and is also crucial in pollution assessment. Here we report the use of industrial image analysis techniques to visualise for the first time individual peptide/DNA particles in physiological aqueous solution. This enables a precise assessment of individual particle size and shape in solution, and an accurate measurement of particle number. Analysis of these parameters in particles formed with eight different (Lys)<sub>16</sub>-containing synthetic peptides has provided interesting new insights for non-viral gene delivery.

## 2. Materials and methods

### 2.1. Peptides

Synthesis, cyclisation via cysteine residues (where indicated) and purification by HPLC techniques were performed by Cambridge Research Biochemicals (Northwich, Cheshire, UK). The peptides were supplied as a dried powder and stored desiccated at  $-35^{\circ}\text{C}$ .

### 2.2. Formation of peptide/DNA particles

Polymol/DNA nanoparticles were prepared at a weight/weight (w/w) ratio of 3:1, polymol powder (as supplied)/DNA, which has previously been shown to be optimal for *in vitro* gene delivery with this vector [6]. This represents an actual polymol peptide/DNA w/w ratio of 2:1, and corresponds to a + to – charge ratio of 2.8:1. All other peptide/DNA particles were formed at this charge ratio.

The plasmids used in the complexes were the pGL2 and pGL3 plasmids (Promega, Madison, WI, USA). These contain 6.046 and 5.256 kb and have molecular weights of  $4 \times 10^6$  and  $3.5 \times 10^6$  Da, respectively. The concentration of DNA was always 10  $\mu\text{g/ml}$ .

The required volume of stock DNA at 1 mg/ml in water was added to PBS in a 15-ml Falcon tube (Helena Biosciences, Sunderland, Tyne and Wear, UK). The required volume of peptide at 1 mg/ml in PBS (to give the required + to – charge ratio of 2.8:1) was added dropwise to the DNA solution while vortexing. This was allowed to stand for 30 min before beginning measurements or adding to target cells for gene delivery. For gene delivery studies, the peptide/DNA particles were formed in culture medium without supplements.

### 2.3. Size characterisation of peptide/DNA nanoparticles using DLS

DLS measurements were performed on a Zetasizer 3000 HS (Malvern Instruments Ltd, Malvern, UK). The z-average diameters and polydispersity index values of peptide/DNA nanoparticles were calculated according to the International Standard on Photon Correlation Spectros-

copy (PCS) [16]. At least three measurements were taken for each sample.

### 2.4. Imaging and measurement of individual peptide/DNA nanoparticles in solution with the Flow Particle Image Analyser

Automated image analysis of peptide/DNA particles in solution was performed on an FPIA 2100 (Sysmex Corporation, Kobe, Japan) [17]. Particles in suspension pass through a sheath flow cell that transforms the particle suspension into a narrow or flat flow, ensuring the largest area of the particle is orientated towards the camera and that all particles are in focus. A CCD microscope illuminated by a stroboscope captures particle images at 30 Hz. The instrument used in these studies uses a pulsed xenon light source which produces white light, giving a lower size detection limit of 0.7  $\mu\text{m}$ . Numerical evaluation of particle shape is derived from measurement of the area of the particle. From this can be determined its perimeter, circularity (defined as the ratio of the perimeter of a circle of equivalent projected area to the perimeter of the particle itself), and diameter (defined as the diameter of a circle of equivalent projected area).

### 2.5. Integrin-binding assay

One hundred microliters of (Lys)<sub>16</sub> peptide at 5  $\mu\text{g/ml}$  in PBS was added to individual wells of a 96-well plate and this was incubated overnight at  $4^{\circ}\text{C}$ . After washing and blocking residual protein-binding sites with 2% bovine serum albumin (BSA), 100  $\mu\text{l}$  of human integrin/mouse Fc fusion protein (kindly supplied by Bernie Sweeney, Cell-Tech, Slough, Middlesex) [18] at 200 ng/ml was added to the wells. After 1 h at room temperature, the plate was washed and 100  $\mu\text{l}$  of peroxidase-labelled goat anti mouse Fc (Jackson Immuno Research, West Grove, PA, USA) was added. After 1 h at room temperature, the plate was washed and 100- $\mu\text{l}$  TMB One Solution (Promega) was added per well. The plate was read at 630 nm after 5 min.

### 2.6. Monoclonal antibodies

A fluorescein-labelled mouse IgG1 antibody specific for the human CD51/CD61  $\alpha\text{v}\beta_3$  integrin heterodimer (Pharmingen, BD Biosciences, San Diego, CA, USA) was used. The control antibody was a fluorescein-labelled mouse IgG1 antibody to human CD90 (Serotec, Oxford, UK).

### 2.7. Cell lines

The HepG2 line (European Collection of Cell Cultures, Salisbury, Wiltshire, UK) and the HUH7 line (from Dr David Crabb, Indiana University Medical Centre, Indianapolis, USA) are adherent lines originally derived from human hepatocyte carcinomas. The ECV304 cell line (European Collection of Animal Cell Cultures) is an adherent

Table 1  
The (Lys)<sub>16</sub>-containing synthetic peptides used in this study

Peptide	Amino acid sequence*	Molecular Weight (Daltons)	Net Charge
Polymol	KKKKKKKKKKKKKKKKKICRRARGDNPDDRCT	3797	+17
PolyRGE	KKKKKKKKKKKKKKKKKICRRARGENPDDRCT	3813	+17
Serine Loop	KKKKKKKKKKKKKKKKKSCSSSSSSSSSSSCS	3407	+16
Linear Polymol	KKKKKKKKKKKKKKKKKIGRRARGDNPDDRGT	3707	+17
PAT1	KKKKKKKKKKKKKKKKKFKNPKPFVFLI	3175	+17
PAT2	KKKKKKKKKKKKKKKKKCSIPPEVKFNPKPFVFLI	4030	+17
(Lys) <sub>16</sub>	KKKKKKKKKKKKKKKKK	2069	+16
(Lys-Pro) <sub>16</sub>	KPKPKPKPKPKPKPKPKPKPKPKPKPKPKPKPK	3622	+16

\*One-letter code. Polymol, PolyRGE and Serine Loop are circularised via the cysteine residues.

human line derived from the bladder carcinoma. They were maintained under mycoplasma-free conditions in Dulbeccos Minimal Essential Medium (DMEM; Invitrogen, Paisley, Scotland) supplemented with 10% heat-inactivated fetal calf serum (FCS), 2 mM glutamine and 1 × Non Essential Amino Acids (Invitrogen), which will be referred to as the culture medium. The HMEC human vascular endothelial cell line (from Professor Marlene Rose, Harefield Hospital, Middlesex) was maintained in MCDB<sub>131</sub> medium (Gibco)

supplemented with 10% FCS, 10 mM L-glutamine, 10 ng/ml endothelial cell growth factor (Sigma) and 1 µg/ml hydrocortisone (Sigma).

## 2.8. Flow cytometry

Cells were harvested by scraping, centrifuged at 200 × g for 10 min at 4 °C and resuspended to 4 × 10<sup>6</sup>/ml in ice-cold 0.5% BSA in PBS. All subsequent procedures were

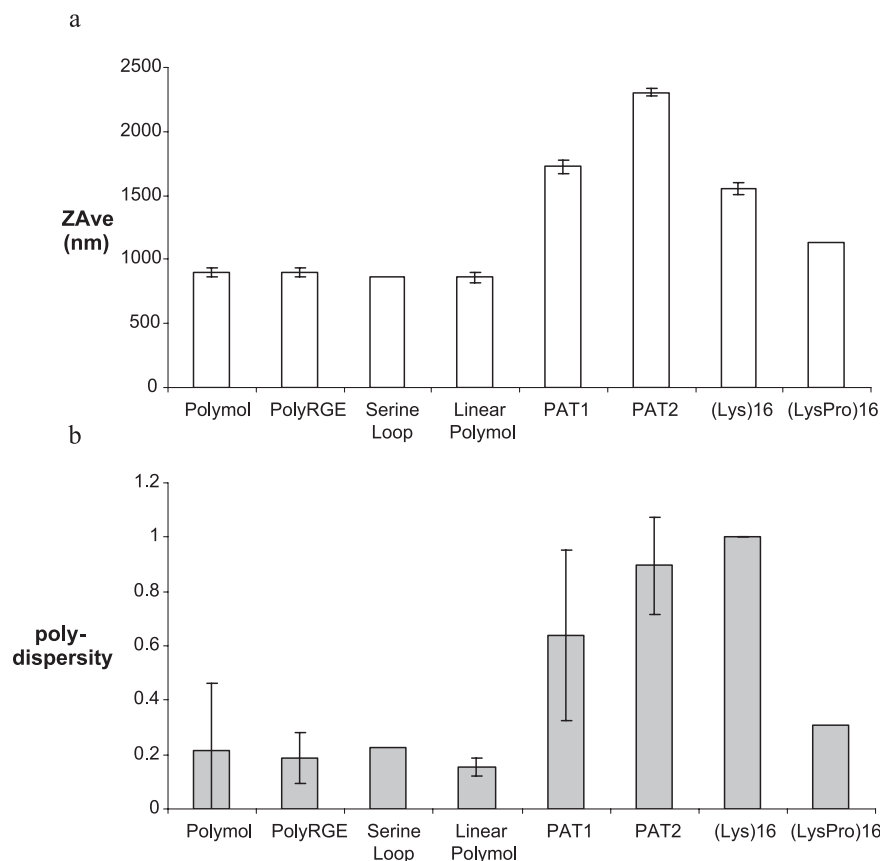


Fig. 1. DLS characterisation of peptide/DNA particles. The z-average (ZAve) diameters (a) and polydispersities (b) of peptide/DNA particles formed at 10 µg/ml of pGL2 DNA in PBS. The peptides (details in Table 1) were used at a constant + to – charge ratio of 2.8:1. For polymol/DNA, this represents w/w ratio of 2:1.

performed on ice or at 4 °C, as previously described (e.g. Refs. [6,9]) and the cells analysed on a FACSCalibur (Becton Dickinson UK Ltd, Oxford, UK).

### 2.9. Transfection of cell lines

Cells were harvested with trypsin/EDTA, pelleted by centrifugation, and resuspended to  $5 \times 10^4$  cells/ml in culture medium. One milliliter of the cell suspension was added to each well of a 24-well plate (Helena Biosciences), and cultured overnight at 37 °C in 95% air/5% CO<sub>2</sub>. Transfection, harvesting of cells after 48 h, and assessment of luciferase expression have been described previously in detail (e.g. Refs. [6,9]).

## 3. Results

The eight (Lys)<sub>16</sub>-containing synthetic peptides used in this study are listed in Table 1.

Polylysine-molossin (*Polymol*) contains the 15-amino-acid, integrin-binding domain of the venom of the American

pit viper, *Crotalus molossus molossus*, and has been used extensively for gene delivery in vitro [4–9] and in vivo [10,11].

*PolyRGE* has precisely the same sequence as *polymol*, except for an aspartate to glutamate substitution in the critical RGD integrin-binding motif [19]. This has been shown to eliminate integrin-binding [20].

The *Serine Loop* peptide has the same overall structure as *polymol*, but the amino acids in the integrin-binding domain (except the two cysteines required for cyclisation) have been replaced by serines.

*Linear polymol* has the same sequence as *polymol*, except that the two cysteine residues have been replaced by glycines to prevent cyclisation.

*PAT1* and *PAT2* contain the FVFLI sequence from human alpha1-antitrypsin for binding to the serpin-enzyme complex receptor (SECR) [21]. These peptides contain a short or a long segment of the alpha1-antitrypsin sequence, and have been evaluated for in vitro gene delivery [8].

(Lys)<sub>16</sub> is the control cationic moiety, without a targeting ligand.

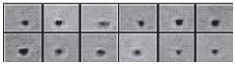
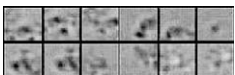
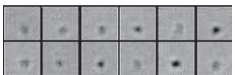
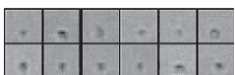
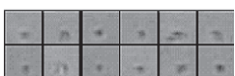
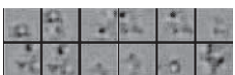

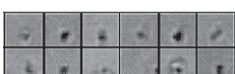
Peptide in complexes	Photograph of particles	Mean diameter (μm)	Mean circularity	Number of complexes per ml
Polymol		0.8	0.766	$2.1 \times 10^7$
(lys) <sub>16</sub>		1.9	0.629	$1.3 \times 10^6$
PolyRGE		0.82	0.831	$8.4 \times 10^6$
Linear Polymol		0.79	0.830	$9.0 \times 10^6$
Serine Loop		0.87	0.745	$7.5 \times 10^6$
PAT1		2.36	0.603	$7.0 \times 10^5$
PAT2		1.47	0.643	$2.0 \times 10^6$
(Lys-Pro) <sub>16</sub>		1.1	0.659	$4.5 \times 10^6$

Fig. 2. Imaging and measurement of individual peptide/DNA particles using Flow Particle Image Analysis (FPIA). Peptide/DNA particles were formed at 10 μg/ml of pGL2 DNA in PBS and at a constant + to – charge ratio of 2.8:1. Peptides are listed in Table 1. For each set of particles, photographs of 12 randomly selected nanoparticles are given. The mean diameter and the mean circularity, based on the assessment of >500 particles, and the number of particles per milliliter are also given. The diameter given for each particle is that of a circle of equivalent projected area. Circularity is a measure of shape and is defined as the ratio of the perimeter of a circle of equivalent projected area to the perimeter of the particle itself.

(Lys-Pro)<sub>16</sub> is a peptide with 16 lysines and no targeting ligand, but with a proline residue alternating with the lysine residues.

### 3.1. Assessment of peptide/DNA nanoparticles using conventional dynamic light-scattering

The results in Fig. 1a demonstrate a remarkably large variation in Z<sub>Ave</sub> for the eight peptide/DNA nanoparticles, even though all were formed at the same charge ratio and using the same DNA concentration and buffer conditions. It is particularly noteworthy that the untargeted (Lys)<sub>16</sub>/DNA particles, frequently used as controls for targeted vector/DNA particles, have a much larger Z<sub>Ave</sub> than polymol/DNA particles. Clearly, the addition of a small peptide to (Lys)<sub>16</sub> greatly influences its DNA-condensing properties. The PAT1 and PAT2 peptides targeted to the SECR form peptide/DNA particles with a Z<sub>Ave</sub> larger than untargeted (Lys)<sub>16</sub> peptide/DNA nanoparticles. This finding introduces a previously unrecognised variable for interpreting the use of untargeted polylysines as controls for targeted polylysines: any difference in transfection efficiency might as easily be a consequence of the different physical properties of the particles, as of the presence or absence of targeting ligands.

Table 2

Number of DNA plasmids per peptide/DNA nanoparticle

Peptide	DNA (ml <sup>-1</sup> )		Nanoparticles (ml <sup>-1</sup> ) <sup>b</sup>	Plasmids per nanoparticle
	μg	Plasmids <sup>a</sup>		
Polymol	10	$1.5 \times 10^{12}$	$2.1 \times 10^7$	71,000

<sup>a</sup> pGL2 plasmid (6.046 kb) of molecular weight  $4.0 \times 10^6$  Da. The molecular weight in grams is equivalent to 1 mol, which contains  $6.022 \times 10^{23}$  molecules (Avogadro's number). Therefore, 4.0 μg contains  $6 \times 10^{11}$  plasmids.

<sup>b</sup> Polymol/DNA complexes formed at 10 μg/ml of pGL2 DNA in PBS and at a + to – charge ratio of 2.8 to 1. See Fig. 2.

Measurement of polydispersity, a parameter related to the uniformity of particle size (Fig. 1b), shows that the particles with the larger Z<sub>Ave</sub> measurements were the least uniform in size.

### 3.2. Assessment of peptide/DNA nanoparticles by direct imaging of individual particles in physiological aqueous solution using a Fluid Particle Image Analyser (FPIA)

This technique enables not only a much more precise assessment of the physical properties of the particles, but does so in physiological solutions identical to those in

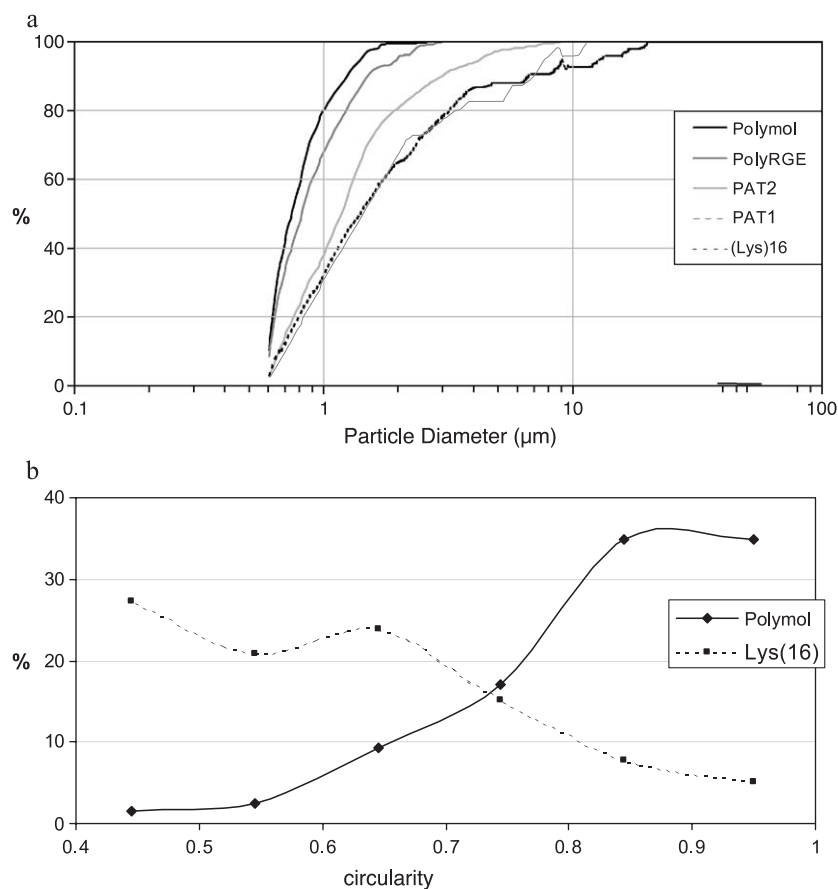


Fig. 3. Measurement of size and shape of individual peptide/DNA particles. Peptide/DNA particles were formed at 10 μg/ml of pGL2 DNA in PBS and at a constant + to – charge ratio of 2.8:1. Peptides are listed in Table 1. Cumulative size distribution (a) and circularity distribution (b) are based on individual measurements of >500 particles. Particle diameter and circularity as defined in the legend to Fig. 2.

which peptide/DNA particles interact with target cells during gene delivery.

Fig. 2 shows, for the first time, photographs of individual peptide/DNA nanoparticles in physiological aqueous solution. It can be seen that polymol/DNA complexes form regular, spherical nanoparticles with an average diameter of 0.8  $\mu\text{m}$ . Interestingly, when larger particles occasionally were seen, they appeared as multiples (usually 2 or 3) of the smaller particles. The (Lys)<sub>16</sub>/DNA complexes, by contrast, form irregularly shaped, larger and looser-looking structures of average diameter 1.9  $\mu\text{m}$ , and with  $\sim 20$ -fold

fewer particles/ml. Particles formed with PolyRGE, Linear Polymol and the Serine Loop peptides look very similar to those formed with polymol. Particles with PAT1 and PAT2, on the other hand, look similar to those formed with (Lys)<sub>16</sub>. The picture with (Lys-Pro)<sub>16</sub> particles is similar to that seen with polymol, but less compact.

The ability to assess particles individually enables an accurate profile of size distribution (Fig. 3a) and shape distribution (Fig. 3b). For example, in the case of particles formed with polymol, 80% are smaller than 1  $\mu\text{m}$  in diameter, and none is larger than 2  $\mu\text{m}$  in diameter. In the

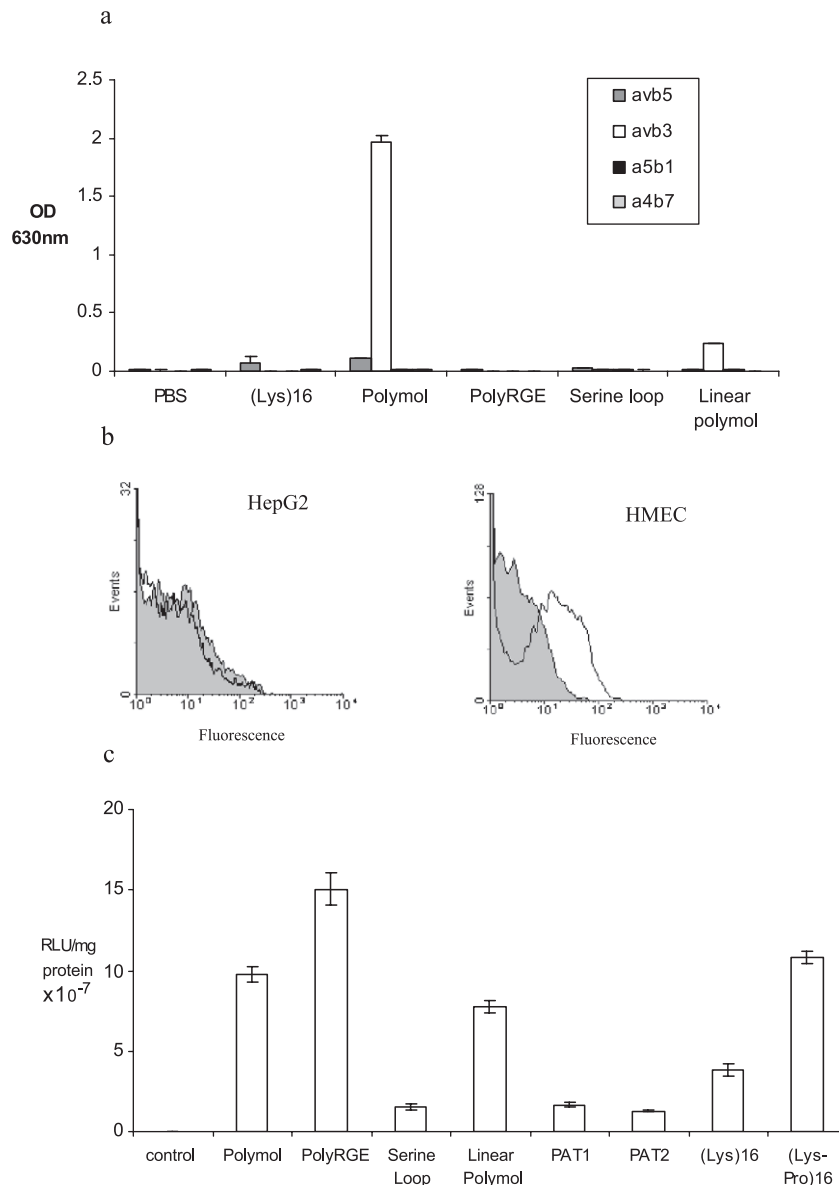


Fig. 4. Target cell characterisation and integrin-independent gene delivery studies. (a) Binding of recombinant human integrin/mouse Ig fusion proteins (as indicated on the figure) to immobilised peptides was analysed on 96-well plates. The Optical Density (OD) at 630 nm refers to peroxidase-labelled goat anti-mouse Ig. (b) Flow cytometry using the control antibody (shaded) and the antibody to  $\alpha\text{v}\beta_3$  integrins (line) on HepG2 and HMEC lines. Results with HUH7 were similar to HepG2 (not shown). (c) The HepG2 cell line was transfected with the peptide/DNA complexes indicated, at a constant + to - charge ratio of 2.8:1. The pGL3 plasmid was used at a concentration of 10  $\mu\text{g}/\text{ml}$  of DNA. In the absence of chloroquine (control), none of the complexes gave measurable gene delivery. Chloroquine at 100  $\mu\text{M}$  was included in all other transfections. Reporter gene expression is given as RLU per milligram of protein. Values are means  $\pm$  S.E. of triplicates.



case of particles formed with (Lys)<sub>16</sub>, only 30% are smaller than 1  $\mu\text{m}$ , and  $\sim 10\%$  are aggregates larger than 10  $\mu\text{m}$  (Fig. 3a). Whereas the large majority of particles formed with polymol conform to an approximately spherical shape (circularity  $>0.8$ ), this is the case for only a small minority of particles formed with (Lys)<sub>16</sub> (Fig. 3b).

Although current FPIA instrumentation has a lower detection limit of 700 nm (please refer to Section 2), the DLS analysis excludes the possibility that there is a significant component of smaller particles.

### 3.3. Multiplicity of infection/transfection

A critical parameter for gene delivery by virus vectors is the Multiplicity of Infection (MOI), i.e. the number of virus particles per target cell in the transfection medium. It has hitherto not been possible to calculate the corresponding number (perhaps the Multiplicity of Transfection) for non-viral gene delivery systems. A typical transfection involves 0.3 ml of peptide/DNA particles added to a well containing  $10^5$  cells. One can therefore calculate (from particle concentrations given in Fig. 1) that there are  $\sim 60$  polymol/DNA nanoparticles per cell. By contrast, with (Lys)<sub>16</sub>/DNA particles, there are only four nanoparticles per cell. Thus, in addition to their much larger size and irregular shape, there are many fewer (Lys)<sub>16</sub>/DNA nanoparticles in comparison with polymol/DNA nanoparticles at the same DNA concentration.

### 3.4. The number of plasmids per peptide/DNA nanoparticle

An interesting parameter is the number of DNA plasmids per particle. As demonstrated in Table 2, for polymol/DNA particles formed under standard conditions, there are  $\sim 70,000$  plasmids per particle. This calculation assumes that all or most of the DNA in solution is condensed into

particles on addition of polymol. Certainly, as shown by gel retardation assays, all the DNA in solution reacts with the (Lys)<sub>16</sub> peptides to a point of electroneutrality [6].

### 3.5. The variable physical properties of (Lys)<sub>16</sub>-containing peptides influence the efficiency of gene delivery

The objective of these studies was to see if there is a relationship between the physical properties of the (Lys)<sub>16</sub>-containing peptide/DNA particles and their capacity for gene delivery. To strictly compare the gene delivery properties of the eight peptide/DNA particles in this study, it is critical to exclude receptor-targeting as a potential contributor to the efficacy of gene delivery. Otherwise, targeted particles will have a potential advantage, unrelated to their physical properties.

Molossin, the integrin-binding domain of which is incorporated into polymol, binds to several integrins, but in particular to  $\alpha\text{v}\beta_3$  [22]. The binding of polymol and the other peptides to several integrins was tested using purified recombinant integrins. The results in Fig. 4a show that polymol binds strongly to  $\alpha\text{v}\beta_3$  integrin, very weakly to  $\alpha\text{v}\beta_5$  integrin, but not at all to  $\alpha_5\beta_1$  and  $\alpha_4\beta_7$  integrins. Cyclisation via cysteines is believed to stabilise the integrin-binding domain [23], and it was therefore interesting to see that Linear Polymol bound only weakly to  $\alpha\text{v}\beta_3$  integrins, and not at all to other integrins. PolyRGE, as predicted [20], does not bind to integrins. We therefore sought a cell line lacking  $\alpha\text{v}\beta_3$  integrins for the gene delivery experiments.

The results in Fig. 4b demonstrate that the HepG2 hepatocyte cell line does not express  $\alpha\text{v}\beta_3$ , but the HMEC endothelial cell line does express this integrin. The HUH7 hepatocyte cell line does not express  $\alpha\text{v}\beta_3$  integrins, while the ECV line does express these integrins (data not shown). The HepG2 cell line was used for the gene delivery studies in this section.

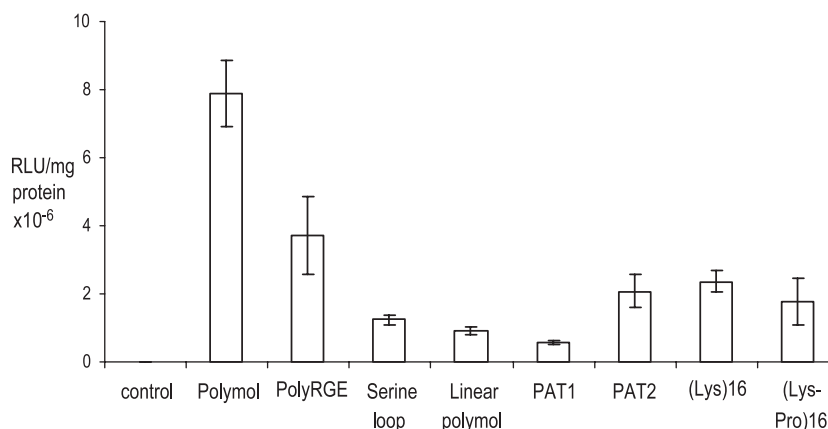


Fig. 5. Gene delivery to a cell line with cell surface integrin receptors. The ECV cell line was transfected with the peptide/DNA complexes indicated at a constant + to – charge ratio of 2.8:1, and the pGL3 plasmid at a concentration of 10  $\mu\text{g}/\text{ml}$  of DNA. In the absence of chloroquine (control), none of the complexes gave measurable gene delivery. Chloroquine at 100  $\mu\text{M}$  was included in all other transfections. Reporter gene expression is given as RLU per milligram of protein. Values are means  $\pm$  S.E. of triplicates.

The results given in Fig. 4c demonstrate a large variability between the peptides in their capacity for gene delivery. The prototype polymol/DNA particles are unlikely to have any targeting advantages on the HepG2 cell line, and it is interesting that the polyRGE/DNA particles and the (Lys-Pro)<sub>16</sub>/DNA nanoparticles were as effective, or slightly more effective, than polymol/DNA particles for gene delivery. Linear Polymol gave results similar to Polymol. These four peptides all produced small, spherical particles (Fig. 2). The large and irregular (Lys)<sub>16</sub>, PAT1 and PAT2 peptide/DNA particles, with relatively few particles per milliliter, all gave poor gene delivery. The physical properties of the Serine Loop peptide/DNA particles were very similar to the polymol/DNA nanoparticles, but gene delivery with this vector was poor.

### 3.6. The influence of integrin-targeting on the efficiency of gene delivery

We investigated this by transfecting the ECV cell line using the eight (Lys)<sub>16</sub>-containing peptides as vectors. In contrast to the HepG2 cell line, polylysine-molossin had a >2-fold greater capacity for gene delivery when compared to the other peptides (Fig. 5). This is consistent with the idea that integrin-targeting contributes to the efficiency of gene delivery where the target cell carries the appropriate integrin-receptors. However, substantial gene delivery can occur independently of specific receptor-targeting.

## 4. Discussion

Flow Particle Image Analysis (FPIA) is a technique normally used for the detection, characterisation and quantitation of particles in industrial and environmental fluids, for reasons of quality control and pollution assessment. This technique gives precise measurements of particle size and shape, and provides accurate particle counts. We have used it to visualise individual (Lys)<sub>16</sub>-containing peptide/DNA particles in physiological aqueous solutions.

Our major finding is that the “targeting” moiety of (Lys)<sub>16</sub>-containing, bifunctional synthetic peptides greatly influences the physical properties of the peptide/DNA particles. Untargeted (Lys)<sub>16</sub> peptides form large, loosely structured and irregular particles, with relatively few particles per milliliter. For reasons which are not clear, adding the 15-amino-acid integrin-binding loop of molossin results in smaller, more compact, and more numerous spherical particles. This is not a consequence of the presence of a cyclised loop, as the Linear Polymol gives equally good particles. Moreover, it is not a consequence of the presence of charged residues in the targeting moiety, as the Serine Loop peptide also forms excellent particles. On the other hand, the addition of small peptides to (Lys)<sub>16</sub> can also increase the size of peptide/DNA particles, as seen with the PAT1

and PAT2 peptides containing the hydrophobic, SECR-binding FVFLI sequence. The spacing of the lysines, or perhaps secondary structure of the peptides, might also influence the quality of nanoparticles, given that (Lys-Pro)<sub>16</sub>/DNA nanoparticles are very different from (Lys)<sub>16</sub>/DNA particles.

Comparisons of gene delivery efficiency are frequently made between targeted and untargeted polycations, in order to infer receptor-specificity of gene delivery. Our studies demonstrate that differences in efficacy of gene delivery might be a consequence of differences in the physical properties of the vector/DNA particles, rather than on the presence or absence of targeting per se. For example, we have previously reported a ~ 2-fold advantage for gene delivery with polylysine-molossin as compared to (Lys)<sub>16</sub> peptide/DNA complexes on target cells not characterized for integrin expression (e.g. Refs. [4,6]). In this report, we compare polylysine-molossin with the non-integrin-binding RGE peptide and (Lys)<sub>16</sub> peptide/DNA complexes on integrin-positive and integrin-negative cell lines. Clearly, simple comparisons of polylysine-molossin and (Lys)<sub>16</sub> are of no value for inferring receptor-specificity of gene delivery. However, the twofold greater efficacy of polylysine-molossin as compared to the RGE peptide on the integrin-positive cell line suggests a contribution of receptor-targeting for gene delivery.

The poor gene delivery with the Serine Loop peptide was interesting, given that it condensed plasmid DNA into what looked like excellent peptide/DNA particles. There is no obvious explanation at the moment, but there are many possibilities such as absence of nuclear localisation properties [24].

The ability to measure accurately the number of vector/DNA particles in physiological aqueous solutions reveals that, under standard conditions of gene delivery, ~ 60 polymol/DNA particles are present per cell. This represents a high “Multiplicity of Infection/Transfection”, as efficient gene delivery can frequently be obtained by viral vectors at lower MOIs. Moreover, each particle probably contains ~ 70,000 DNA plasmids. By contrast, virus particles usually contain only one, sometimes two, copies of their genome. However, viruses harbour elaborate mechanisms for carefully shepherding their genome into the nucleus [25]. A single virus particle delivering a single genome to a target cell can usually effectively infect that cell. Peptide/DNA particles appear to “flood” the cell with a multitude of unprotected plasmids. Similarly, Labat-Moleur et al. [15] estimated from electron microscopy of transfected cells that each contained several hundred cationic lipid/DNA nanoparticles.

We have performed this analysis with peptide/DNA particles in physiological aqueous solutions, because these are the biologically relevant solutions in which peptide/DNA particles interact with target cells. In these solutions, polylysine/DNA particles have diameters of several hundred nanometers, which is much larger than can be accommodated by classical endocytic vesicles [26]. The precise



pathway of intracellular delivery is uncertain, and is being investigated using ultrastructural techniques. One possibility is internalization via phagocytic-type mechanisms. It is known that these can be activated in many epithelial cells by certain membrane proteins of obligate intracellular bacteria (e.g. invasins of *Yersinia pseudotuberculosis*) [27].

Using DLS techniques, it is known that peptide/DNA particles are much smaller in nonionic, isotonic solutions such as 5% dextrose in water (e.g. Ref. [11]). These smaller particles are below the size limit of detection of the current FPIAs, which is governed primarily by the wavelength of the illuminating light source. The shorter the wavelength of the incident light, the smaller the particles that can be visualized, and it should be possible to design instruments with much smaller detection limits.

The capacity to readily image individual vector/DNA nanoparticles in solution and to count them accurately will enable a more precise assessment of non-viral DNA vectors, and a more quantitative interpretation of gene delivery experiments.

## Acknowledgements

This work was supported by the Biotechnology and Biological Sciences Research Council (Ref Number 29/G14089). We would like to thank CellTech (Slough, Middlesex) for providing the recombinant human integrins.

## References

- [1] D.D. Lasic, N.S. Templeton, Liposomes in gene therapy, *Adv. Drug Deliv. Rev.* 20 (1996) 221–226.
- [2] D. Luo, W.M. Saltzman, Synthetic DNA delivery systems, *Nat. Biotechnol.* 18 (2000) 33–37.
- [3] W. Zauner, M. Ogris, E. Wagner, Polylysine-based transfection systems utilizing receptor-mediated delivery, *Adv. Drug Deliv. Rev.* 30 (1998) 97–113.
- [4] L. Shewring, L. Collins, S.L. Lightman, S. Hart, K. Gustafsson, J.W. Fabre, A nonviral vector system for efficient gene transfer to corneal endothelial cells via membrane integrins, *Transplantation* 64 (1997) 763–769.
- [5] L. Collins, K. Gustafsson, J.W. Fabre, Tissue-binding properties of a synthetic peptide DNA vector targeted to cell membrane integrins: a possible universal nonviral vector for organ and tissue transplantation, *Transplantation* 69 (2000) 1041–1050.
- [6] L. Collins, G.J. Sawyer, X.H. Zhang, K. Gustafsson, J.W. Fabre, In vitro investigation of factors important for the delivery of an integrin-targeted nonviral DNA vector in organ transplantation, *Transplantation* 69 (2000) 1168–1176.
- [7] J.M. Li, L. Collins, X. Zhang, K. Gustafsson, J.W. Fabre, Efficient gene delivery to vascular smooth muscle cells using a nontoxic, synthetic peptide vector system targeted to membrane integrins: a first step toward the gene therapy of chronic rejection, *Transplantation* 70 (2000) 1616–1624.
- [8] S. Patel, X. Zhang, L. Collins, J.W. Fabre, A small, synthetic peptide for gene delivery via the serpin-enzyme complex receptor, *J. Gene Med.* 3 (2001) 271–279.
- [9] X. Zhang, L. Collins, J.W. Fabre, A powerful cooperative interaction between a fusogenic peptide and lipofectamine for the enhancement of receptor-targeted, non-viral gene delivery via integrin receptors, *J. Gene Med.* 3 (2001) 560–568.
- [10] X. Zhang, L. Collins, G.J. Sawyer, X. Dong, Y. Qiu, J.W. Fabre, In vivo gene delivery via portal vein and bile duct to individual lobes of the rat liver using a polylysine-based nonviral DNA vector in combination with chloroquine, *Hum. Gene Ther.* 12 (2001) 2179–2190.
- [11] X. Zhang, G.J. Sawyer, X. Dong, Y. Qiu, L. Collins, J.W. Fabre, The in vivo use of chloroquine for promoting non-viral gene delivery to the liver via the portal vein and bile duct, *J. Gene Med.* 5 (2003) 209–218.
- [12] M.A. Wolfert, L.W. Seymour, Atomic force microscopic analysis of the influence of the molecular weight of poly(L)lysine on the size of polyelectrolyte complexes formed with DNA, *Gene Ther.* 3 (1996) 269–273.
- [13] M.X. Tang, F.C. Szoka, The influence of polymer structure on the interactions of cationic polymers with DNA and morphology of the resulting complexes, *Gene Ther.* 4 (1997) 823–832.
- [14] D. Oupický, C. Konak, K. Ulbrich, M.A. Wolfert, L.W. Seymour, DNA delivery systems based on complexes of DNA with synthetic polycations and their copolymers, *J. Control. Release* 65 (2000) 149–171.
- [15] F. Labat-Moleur, A.M. Steffan, C. Brisson, H. Perron, O. Feugeas, P. Furstemberger, F. Oberling, E. Brambilla, J.P. Behr, An electron microscopy study into the mechanism of gene transfer with lipopolyamines, *Gene Ther.* 3 (1996) 1010–1017.
- [16] Methods for determination of particle size distribution; Part 8: photon correlation spectroscopy, ISO number 13321, <http://www.iso.com>, International Standards Organisation (ISO) 13321 (1996).
- [17] Apparatus and method for analysing particle images, including measuring at a plurality of capturing magnifications, US Patent 5,721,433 (2003).
- [18] P.E. Stephens, S. Ortlepp, V.C. Perkins, M.K. Robinson, H. Kirby, Expression of a soluble functional form of the integrin  $\alpha 4 \beta 1$  in mammalian cells, *Cell Adhes. Commun.* 7 (2000) 377–390.
- [19] E. Ruoslahti, M.D. Pierschbacher, New perspectives in cell adhesion: RGD and integrins, *Science* 238 (1987) 491–497.
- [20] N. Greenspoon, R. Hershkovich, R. Alon, D. Varon, B. Shenkman, G. Marx, S. Federman, G. Kapustina, O. Lider, Structural analysis of integrin recognition and the inhibition of integrin-mediated cell functions by novel nonpeptidic surrogates of the Arg-Gly-Asp sequence, *Biochemistry* 32 (1993) 1001–1008.
- [21] G. Joslin, R.J. Fallon, J. Bullock, S.P. Adams, D.H. Perlmuter, The SEC receptor recognizes a pentapeptide neodomain of  $\alpha 1$ -antitrypsin-protease complexes, *J. Biol. Chem.* 266 (1991) 11282–11288.
- [22] R.M. Scarborough, J.W. Rose, M.A. Naughton, D.R. Phillips, L. Nannizzi, A. Arfsten, A.M. Campbell, I.F. Charo, Characterization of the integrin specificities of disintegrins isolated from American pit viper venoms, *J. Biol. Chem.* 268 (1993) 1058–1065.
- [23] M.D. Pierschbacher, E. Ruoslahti, Influence of stereochemistry of the sequence Arg-Gly-Asp-Xaa on binding specificity in cell adhesion, *J. Biol. Chem.* 262 (1987) 17294–17298.
- [24] M. Colin, S. Moritz, P. Fontanges, M. Kornprobst, C. Delouis, M. Keller, A.D. Miller, J. Capeau, C. Coutelle, M.C. Brahimi-Horn, The nuclear pore complex is involved in nuclear transfer of plasmid DNA condensed with an oligolysine-RGD peptide containing nuclear localisation properties, *Gene Ther.* 8 (2001) 1643–1653.
- [25] M.A. Kay, J.C. Glorioso, L. Naldini, Viral vectors for gene therapy: the art of turning infectious agents into vehicles of therapeutics, *Nat. Med.* 7 (2001) 33–40.
- [26] S.D. Connor, S.L. Schmid, Regulated portals of entry into the cell, *Nature* 6 (2003) 37–44.
- [27] R.R. Isberg, J.M. Leong, Multiple  $\beta 1$  chain integrins are receptors for invasins, a protein that promotes bacterial penetration into mammalian cells, *Cell* 60 (1990) 861–871.